Acta Polytechnica **64**(4):341–349, 2024
https://doi.org/10.14311/AP.2024.64.0341

Published by the Czech Technical University in Prague

THE LOAD-TRANSFER METHOD AS A TOOL FOR DETERMINING THE LOAD-DISPLACEMENT CURVE OF PILES

Juraj Chalmovský[a,*], Václav Račanský[b], Pavel Koudela[a], Karel Zdražil[a,c]

[a] *Brno University of Technolohy, Faculty of Civil Engineering, Veveří 95, 602 00 Brno, Czech Republic*

[b] *Keller Grundbau Ges.mbH, Guglgasse 15, BT4a/3. OG, 1110 Wien, Austria*

[c] *GEOSTAR, spol. s. r. o., Tuřanka 111, 627 00 Brno, Czech Republic*

[*] corresponding author: chalmovsky.j@fce.vutbr.cz

Abstract. The paper presents two applications (software packages) in which the load-transfer method is used for axially loaded Kelly drilled bored piles and displacement ductile iron piles. In the first, the ultimate friction is related to the effective stress via the so-called β method. The β method is refined into three stages to cover the variety of soils typical of Central Europe. For the driven piles, a different approach is presented in which the ultimate shaft friction is related to the reference hammering time. The recorded hammering time profile is fed directly into the software based on the load-transfer method. Analyses of five loading tests are presented proving that the load transfer method in combination with the β method or the recorded hammering time profile is able to compute the load-displacement curve of both replacement and displacement piles with a reasonable accuracy in various geological conditions.

Keywords: Load-transfer method, deep foundations, pile, ultimate shaft friction, base resistance, load-displacement curve, effective stress.

1. Introduction

The prediction of the load-displacement curve and the ultimate bearing capacity of deep foundations is currently possible using three different approaches:

(1.) Empirical methods – these procedures usually take the form of correlations between design parameters (e.g. the ultimate shaft friction) and results from in-situ or laboratory tests. An example of empirical design procedures is the so-called α method in which the ultimate friction $q_{s,\mathrm{ult}}$ is related to the undrained shear strength.

(2.) Semi-empirical methods – they are often in line with basic principles of soil mechanics. The complexity of these procedures is still low enough to perform the calculation manually. The so-called β method belongs to this group. In this approach, the ultimate shaft friction is related to the effective overburden pressure. Methods for computation of the load-displacement curve based on elasticity theory [1] also belong to this category. Non-linear, plastic soil behaviour that further depends on the loading history and the actual stress state is accounted for by various empirical constants.

(3.) Complex numerical procedures – the load-transfer method, the finite element method, the finite difference method, and the boundary element method in combination with advanced constitutive models belong to this category.

The load-transfer method on which this paper focuses is considered as a complex method. However, it still represents a certain compromise between empirical and semi-empirical methods in the first two categories and more complex numerical procedures in the third category such as the finite element method. Experiences with two types of deep foundations are summarised in this paper:

(1.) Bored large diameter piles – a specialised software was created for this type of deep foundations between 2019 and 2021. The load-transfer method was validated by inverse analyses of more than 30 loading tests in Slovakia, the Czech Republic, and Austria. The number of analysed tests is continuously increasing. The software development, and its validation were carried out in cooperation with the company GEOSTAR.

(2.) Driven ductile iron piles – from 2020 to 2022, the load-transfer method was modified and 28 inverse analyses of loading tests of ductile iron piles were carried out. The loading tests were performed on various construction sites located in Austria and Germany. Modifications of the load-transfer method, software development and its validation were carried out for Keller Grundbau Ges.mbH.

2. Theoretical background of the load-transfer method

The axial load-transfer method (t-z method) introduced by [2] and further modified by [3] and [4] is based on the idea that pile-soil interaction can be replaced by the load-transfer functions (LTF) (mobilisation curves). The load transfer function for the pile shaft is defined as a dependence between the vertical

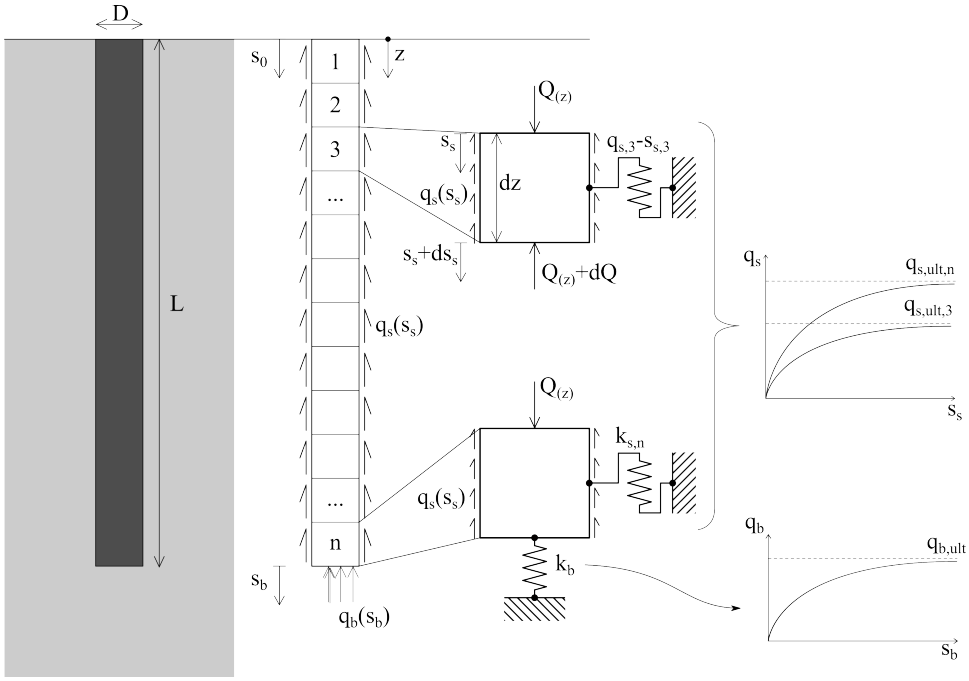

FIGURE 1. Basic principle of the load-transfer method.

displacement of the segment (s_s) and the shear stress mobilised on its surface (q_s). A similar dependency between the normal stress at the pile base (q_b) and the corresponding base displacement (s_b) is added for the pile tip in the case of compressive loads. An analysed deep foundation is divided into a predefined number of segments and an individual load-transfer function is assigned for each of them. In this way, it is possible to consider the change in soil stiffness and ultimate shaft friction due to soil layering and increase in depth. The load-transfer function of the pile base is also assigned to the lower edge of the last segment. The computational kernel is based on a pair of iterative cycles in which the force equilibrium of each segment is found considering the elastic deformation of each segment, see Figure 1. The elastic deformation of each segment depends on its Young modulus E_{seg}, cross-sectional area A_{seg}, and segment length L_{seg}. All three variables can be independent for each segment. The length and modulus of elasticity are usually constant for each segment, and the change in the cross-sectional area of the segment can be used to account for the change in the pile diameter (e.g. due to pile casing). The calculation outputs are:

- The load-displacement curve for a pile and pile base,
- mobilised shaft friction profile along a pile for various loading stages,
- shaft friction utilisation profiles along a pile for various loading stages,
- axial force profiles for various loading stages,
- axial displacement profiles for various loading stages.

Various load-transfer curves for monotonous loading are available in the literature and can be categorised into 4 categories:

- Linear (elastic) curves proposed by e.g. [5] for both the shaft and the pile base. These originally elastic solutions were often complemented by the perfectly plastic segment,
- bilinear (linear elastic perfectly plastic) curves recommended by [6] for the pile shaft in non-cohesive soils,
- multilinear curves proposed by e.g. [7] who used the Menard pressuremeter modulus E_m in their formulations,
- nonlinear curves proposed by e.g. [8], [9], and [10].

Based on the results of multiple inverse analyses, the hyperbolic load-transfer function for the shaft Equation (1) and base Equation (2) proposed by [10] was implemented in the load-transfer method (LTM) algorithm. $q_s(s_s)$ is the mobilised shaft friction for the current vertical shaft displacement s_s; $q_b(s_b)$ is the current value of the normal stress on the pile base mobilised for the base displacement s_b. D_s and D_b are the diameters of the shaft and base, respectively. Strength input parameters are represented by the ultimate shaft $q_{s,\text{ult}}$ and base resistance $q_{b,\text{ult}}$. Stiffness of the load-transfer functions is governed by the initial stiffness parameters M_s (shaft) and M_b (base). The effect of varying input parameters values is illustrated for the pile shaft in Figure 2 ($q_{s,\text{ult}} = 50,\ 100,\ 150\,\text{kPa}$) and in Figure 3 ($M_s = 0.0015;\ 0.0030;\ 0.0045$).

$$q_s(s_s) = \frac{q_{s,\text{ult}} \cdot s_s}{M_s \cdot D_s + s_s}, \tag{1}$$

$$q_b(s_b) = \frac{q_{b,\text{ult}} \cdot s_b}{M_b \cdot D_b + s_b}. \tag{2}$$

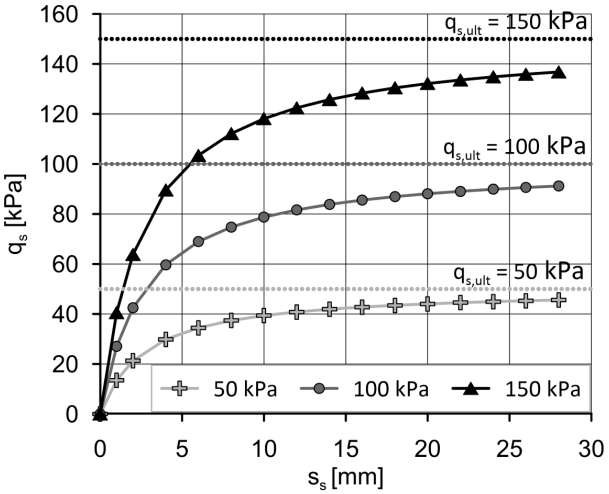

FIGURE 2. Variation of the ultimate shaft friction $q_{s,\mathrm{ult}}$.

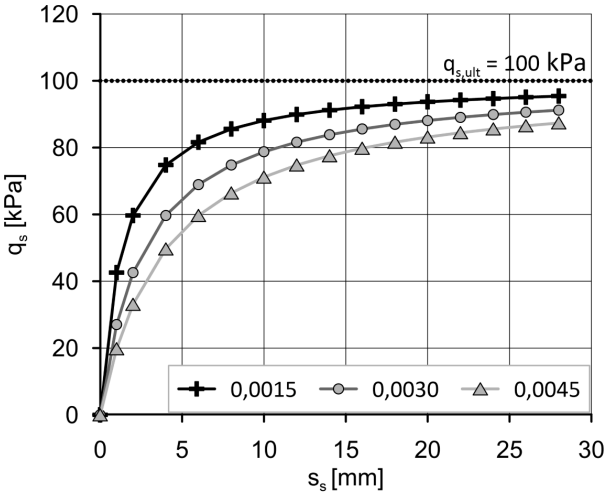

FIGURE 3. Variation of the initial stiffness parameter M_s.

3. Determination of the ultimate shaft friction

In the case of floating piles, it is crucial to define the course of the ultimate shaft friction along a pile. Two different approaches were implemented:

- Bored piles – the ultimate shaft friction depends on the effective overburden stress.
- Driven piles – the ultimate shaft friction is related to the hammering time.

Both approaches are described in more detail in the following chapter and illustrated in Figure 4 and Figure 5.

3.1. Bored piles

The β approach is used. The ultimate shaft friction $q_{s,\mathrm{ult}}$ is related to the effective overburden stress via the β factor Equation (3). This approach is further refined into three stages.

$$q_{s,\mathrm{ult}} = \beta \sigma'_{\mathrm{or}}. \tag{3}$$

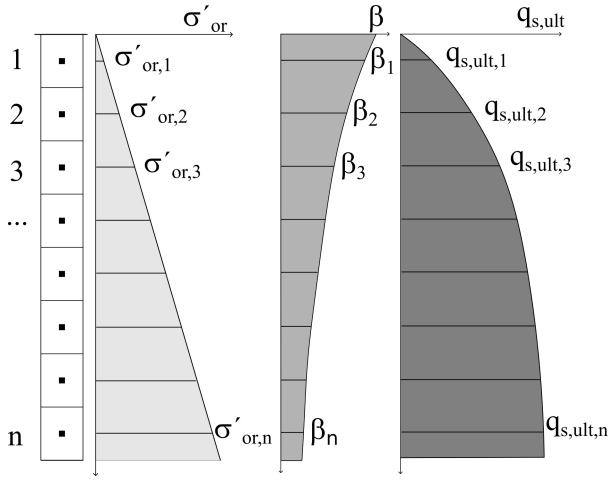

FIGURE 4. Stress-dependent ultimate shaft friction.

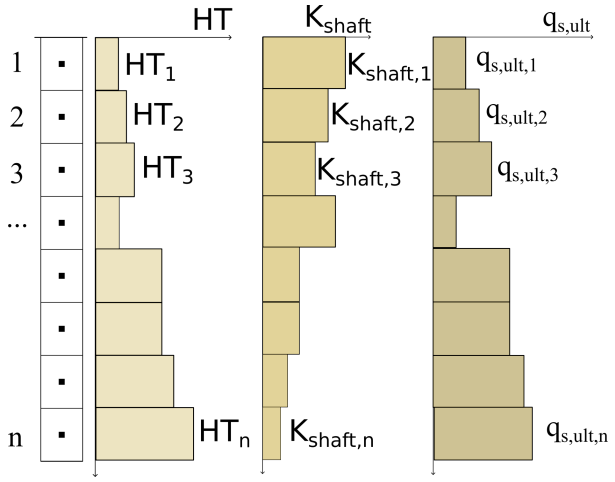

FIGURE 5. Hammering time-dependent shaft friction.

In the 1st stage, the β_{I} factor is stress (depth) independent. This approach is appropriate for normally consolidated cohesive soils, in which the coefficient of lateral pressure K_0 does not depend on depth. Therefore, in our conditions, this approach can be used for the uppermost Quaternary layers. Assuming that $K_0 = 1 - \sin\phi_{\mathrm{cv}}$, the β_{I} factor can be calculated from:

$$\beta_{\mathrm{I}} = K_0 \cdot \tan\phi_{\mathrm{cv}} = (1 - \sin\phi_{\mathrm{cv}}) \cdot \tan\phi_{\mathrm{cv}}, \tag{4}$$

where ϕ_{cv} is the critical state friction angle.

The dependence of the earth pressure coefficient at rest and depth is considered in the 2nd analysis stage. This factor is particularly important in overconsolidated cohesive soils. The β_{II} factor is defined by:

$$\beta_{\mathrm{II}} = (1 - \sin\phi_{\mathrm{cv}}) \left(\frac{POP}{\sigma'_{v,0}} + 1 \right)^{\sin\phi_{\mathrm{cv}}} \tan\phi_{\mathrm{cv}}, \tag{5}$$

where

POP is the preoverburden pressure,

$\sigma'_{v,0}$ is the current overburden stress.

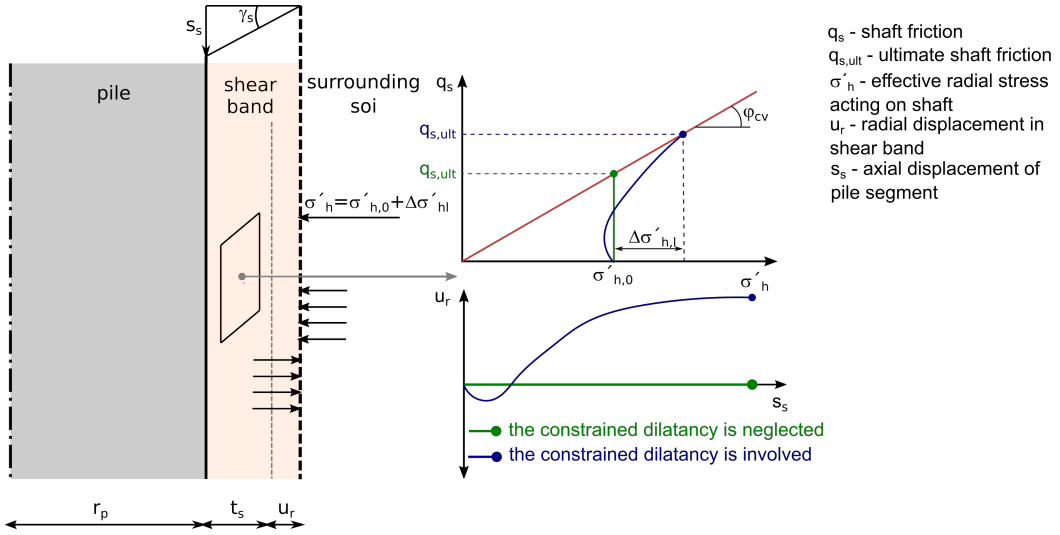

FIGURE 6. Constrained dilatancy effect and its influence on the ultimate shaft friction.

The POP value can be determined from 1D compression tests. Alternatively, correlations with in-situ tests such as CPT can be used. Usually, the expression for the β factor is formulated using the overconsolidation ratio OCR. However, OCR varies with depth, and therefore alternative formulation utilising POP was derived.

In first two stages, it is assumed that the radial stress acting on the pile shaft remains constant during loading. However, in the case of piles constructed in medium dense to dense cohesive soils, the radial stress increases due to the constrained dilatancy effect (Figure 6). Soil inside the shear band located on or in the vicinity of the pile shaft tends to increase its volume (dilate). But this is partially restrained by the influence of the surrounding soil resulting in a radial stress increase $\Delta\sigma_{h,l}$ and thus the ultimate shaft friction increase, 3$^{\text{rd}}$ stage. The β_{III} factor involving this increase can be formulated as:

$$\beta_{\text{III}} = \left((1 - \sin\phi_{\text{cv}}) + \frac{\Delta\sigma_{h,l}}{\sigma'_{v,0}} \right) \tan\phi_{\text{cv}}. \qquad (6)$$

3.2. Driven ductile iron piles

This type of deep foundation is less used compared to bored piles. Therefore, it is briefly described here. A tube made of ductile iron equipped with a shoe is driven into soil using a hydraulic hammer. The concrete is pumped through the tube and holes in the driving shoe during the hammering. In this way, a concrete cover of the ductile iron tube is created. Furthermore, an additional radial displacements of soil is created leading to higher normal stresses acting on the pile shaft and thus a higher available ultimate skin frictions. The fabrication process is schematically shown in Figure 7. The main advantages of this system are: efficiency and speed of production (more than 100 m per day is possible), versatility (tubes can be cut to defined lengths), no heavy machinery is required, ductile iron tubes are produced by recycling waste material.

The hammering times HT_{shaft} required to install each metre of pile are recorded during the pile installation. They reflect the quality of the surrounding soil, and therefore they can be used to estimate the ultimate shaft friction according to Equations (7) and (8). The recorded time profile is transferred to the so-called hammering time in a reference configuration. This time is hereinafter referred as the reference hammering $HT^{\text{ref}}_{\text{shaft}}$ required for driving of 1 m of pile (s m^{-1}). The reference configuration is given by the hammer, driving shoe, and ductile iron tube. $HT^{\text{ref}}_{\text{base}}$ is the reference hammering time needed for driving of the last 10 cm of the pile (s (10 cm)$^{-1}$). K_{shaft} and K_{base} are the load-transfer coefficients for the pile shaft and base, respectively. Their value depends on the soil type and the soil state (consistency or density). The values of these coefficients were derived by an inverse analyses of loading tests, and they continue to be refined.

$$q_{s,\text{ult}} = K_{\text{shaft}} HT^{\text{ref}}_{\text{shaft}}, \qquad (7)$$

$$q_{b,\text{ult}} = K_{\text{base}} HT^{\text{ref}}_{\text{base}}. \qquad (8)$$

4. Application of the load-transfer method for inverse analyses of loading tests

In the following section, the case studies of three loading tests of bored piles and two loading tests of driven ductile iron piles are presented. Results from the first loading test were taken from literature, the remaining four tests are new. The tests took place in the Czech Republic and Austria. All case studies have a form of inverse analyses. The input parameters leading to the best match with measurements are listed in the text. Realness of their values was checked using:

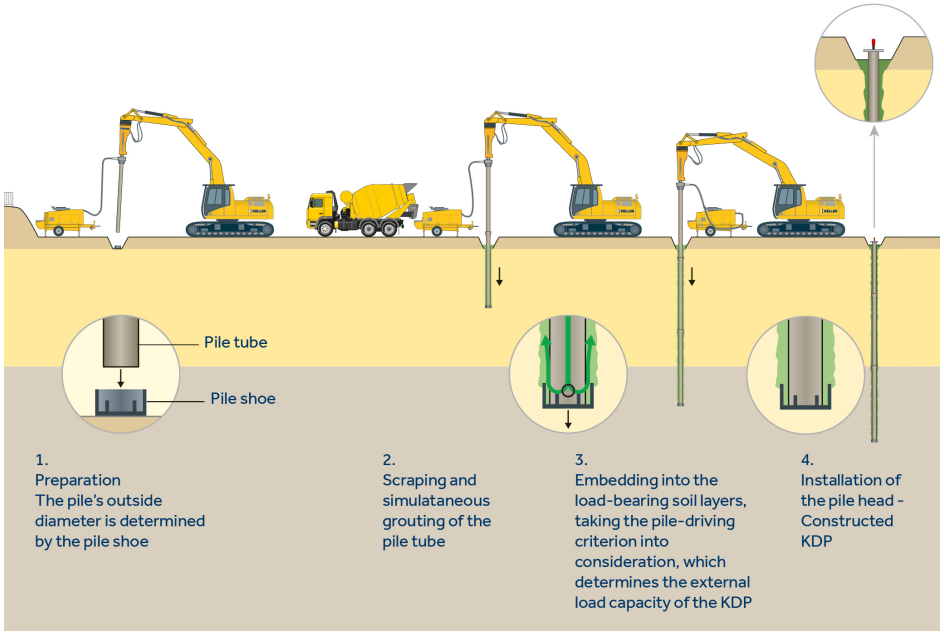

FIGURE 7. Installation process of driven ductile iron pile [11].

(1.) Empirical correlations with in-situ tests (e.g. cone penetration tests),

(2.) data from other authors also using the load transfer method,

(3.) authors' own experience.

4.1. BORED PILES

The first bored pile analysed in this study was constructed as a part of the highway D47 Lipnik nad Becvou-Belotin. It has a length of 15 m and a diameter of 1 200 mm. The bore was cased along its entire length. Quaternary sediments with thicknesses of up to 5 m consist mainly of normally consolidated sandy clay with soft to firm consistency. The pile performance is most affected by the underlying layer of Tertiary overconsolidated clays with a gradually increasing consistency from stiff to hard. The load test was carried out up to a load level of 3 985 kN including three unloading – reloading stages. In addition to the standard force and displacement monitoring in its head, the pile was equipped with electric resistance gauges in five levels [12]. The sufficient displacement induced during the test (29.93 mm) and the knowledge of axial strain and thus shaft friction profiles along the pile from the strain gauges were critical factors in selection of this test for the inverse calculation. A detailed description of all performed analyses is beyond the scope of this paper and is stated in [13]. Only the last analysis with the best results is stated here. Stage I with a constant value of β_{I} factor was adopted for the upper layer of Quaternary sediments. The more advanced Stage II was used for the underlying layer of Tertiary overconsolidated sediments. The final input parameters were as follows: $\beta_{\mathrm{I}}^1 = 0.28$, $M_s^1 = 0.0039$, $POP^2 = 1\,472$ kPa, $M_s^2 = 0.0045$. The upper index denotes the number of the soil layer. The adopted

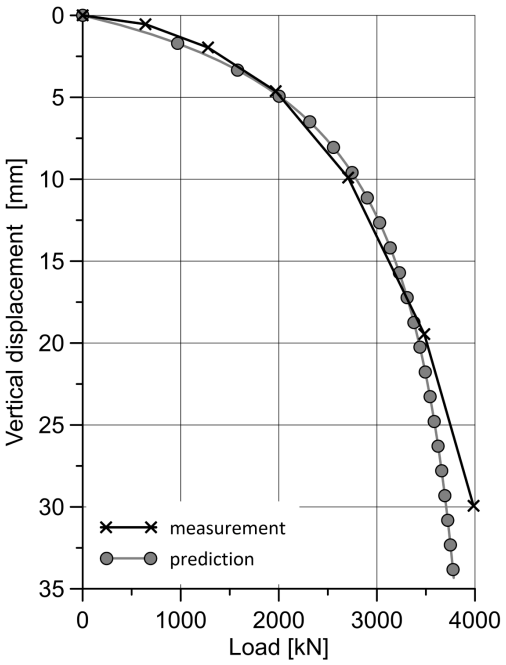

FIGURE 8. Predicted and measured load-displacement curve.

values of stiffness parameters M_s^1 and M_s^2 are consistent with other authors. The value of $M_s = 0.0038$ was recommended regardless of the soil type in the original article [10] in which the currently used formulation of the load-transfer curves was proposed. In [8], hyperbolic curves were also used with a recommended value of M_s equal to 0.0025. The measured and predicted load-displacement curve is shown in Figure 8. Compliance with measurements is sufficient up to a displacement of 20 mm. From this point, the estimated displacements for a given load are slightly higher than measured ones. The ultimate shaft fric-

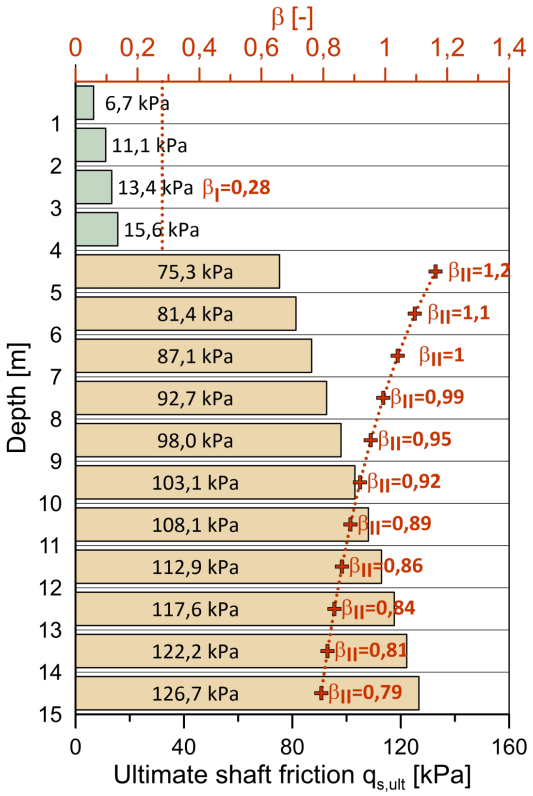

FIGURE 9. Ultimate shaft friction and β factor profiles.

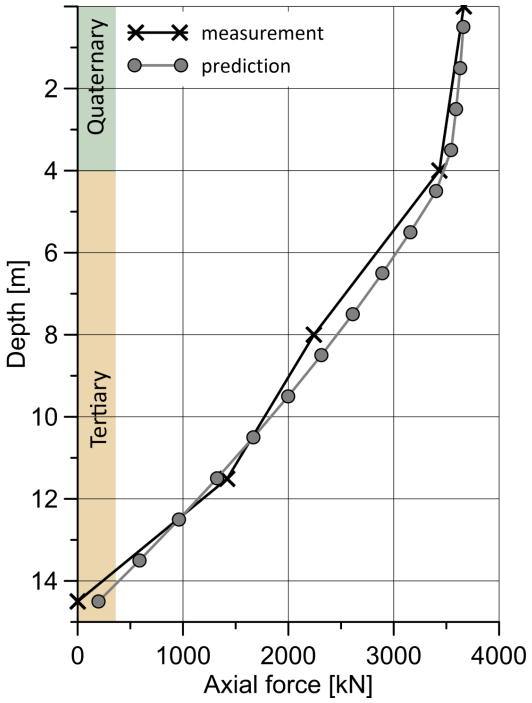

FIGURE 10. Predicted and measured force profile in the last loading stage.

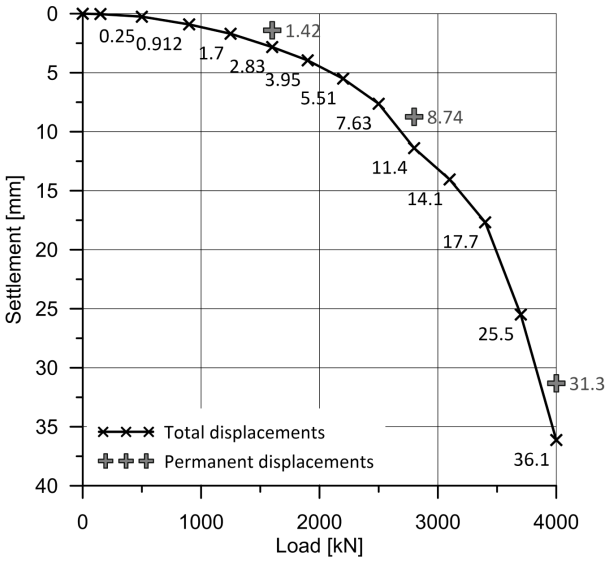

FIGURE 11. Measured load-displacement curves.

tion and β factor profiles along the pile are shown in Figure 9. Recommended values for the ultimate shaft friction of piles in very stiff cohesive soils vary between 85 to 100 kPa [14, 15]. It must be noted that these recommendations include a certain safety margin due to the necessary generalisation. The β factor values in Tertiary overconsolidated clays are significantly higher compared to overlaying Quaternary sediments. This is due to the overconsolidation and thus higher K_0 values. Furthermore, the β factor in overconsolidated soils is not constant, it gradually decreases with depth. This tendency was also determined from multiple pile loading tests in the UK [16]. Measured and predicted axial force profiles for the last loading stage are compared in Figure 10. It is obvious from this figure that the measured decrease in the axial force and thus the mobilised shaft friction are small in the first five meters which is predicted correctly. In the last section of the pile (12.5 to 15 m), the measured shaft friction was slightly higher compared to the predicted one. However, it must be noted, that the measured profile was created by linear interpolation between measured points (position on strain gauges) spaced several metre apart.

Two more loading tests analysed in this study were conducted by the authors in the industrial zone near the city of Ostrava in the north-east part of the Czech Republic. The upper 10.5 m of Quaternary silty clay with local lens of gravelly clay is underlained by Tertiary overconsolidated clay with a stiff to hard consistency with a CPT cone resistance gradually increasing from 6 to 10 MPa. The Stage I and Stage II approaches were applied for the first and second layer, respectively. The first test pile (TP 1) with a length of 17.0 m was loaded to 4 000 kN with a corresponding pile head displacement of 36.1 mm. The load-displacement curve is shown in Figure 11. A relatively high settlement value is sufficient for the application of [17] procedure. The load-displacement curve is transformed from F-u space to u/F-u space (Figure 12). The slope of the linear segment of such a transformed load-displacement curve corresponds to the measured ultimate capacity, $F_{\mathrm{ult,meas}} = 4\,930$ kN. The values of input parameters in the LTM software were as follows: $\beta_{\mathrm{I}}^{1} = 0.27$,

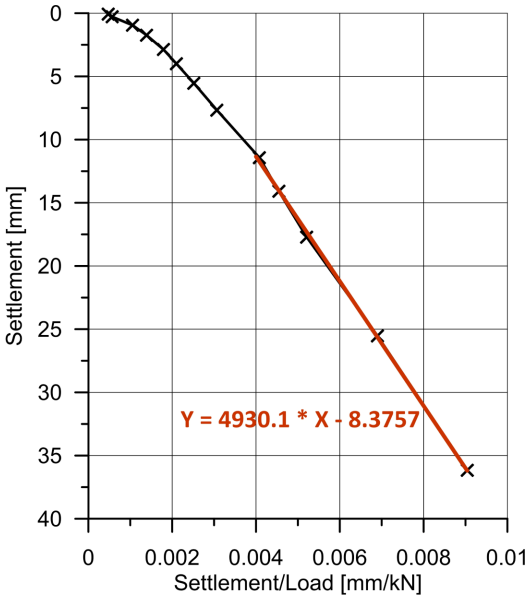

FIGURE 12. Transformed load-displacement curve.

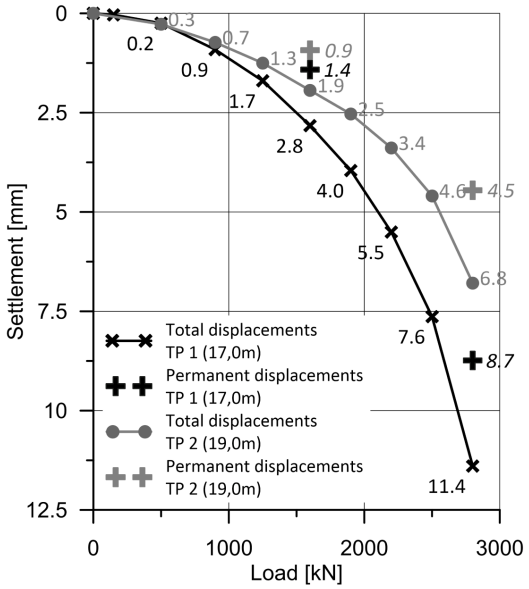

FIGURE 13. Comparison of both measured load-displacement curves.

$M_s^1 = 0.0014$, $POP^2 = 1\,504$ kPa, $M_s^2 = 0.0021$, $q_{b,\mathrm{ult}} = 6\,000$ kPa, $M_b = 0.031$. The predicted shaft and base capacities are $F_{\mathrm{ult,shaft,LTM}} = 2\,379$ kN and $F_{\mathrm{ult,base,LTM}} = 2\,382$ kN , respectively. Thus, the overall predicted capacity $F_{\mathrm{ult,LTM}} = 4\,761$ kN is 3.5 % lower than the measured one. The ultimate shaft friction in the second layer is governed by the pre-overburden pressure. Assuming an initial effective vertical geostatic stress $\sigma_{\mathrm{or}} = 130$ kPa and inversely determined $POP = 1\,501$ kPa leads to the past vertical effective stress $\sigma_p = 1\,631$ kPa. The past vertical effective stress might be estimated from cone penetration tests. Based on the regression analysis, [18] recommended that $\sigma_p = 0.29 q_c$. The value of $q_c = 6$ MPa at a depth with an effective geostatic stress of 130 kPa, which led to the value of $POP = 1.74$ MPa. The same values of input parameters governing the shape of load-transfer curves were further applied for the second load test (TP 2). The second test pile (TP 2) was 2 metres longer ($L_p = 19.0$ m) than the first, but only loaded to 2 800 kN. Both measured load-displacement curves are compared in Figure 13 for the same load levels. Measured load-displacement curves and those predicted for a wider range of settlement are shown in Figure 14. Finally, the ultimate shaft friction and the β factor profile are shown in Figure 15.

4.2. Driven ductile iron piles

Modifications of the standard load-transfer method for ductile driven piles are presented in the inverse analyses of two piles (PP3a, PP3b). These piles were constructed as a part of the testing site Hollern II nearby the city of Vienna. The length of both piles was 9 m. The piles were equipped with conical driving shoes and constructed in stiff clays (Cl). Figure 16 consists of two graphs. The recorded hammering times are ploted in the left part. Assumed ultimate shaft

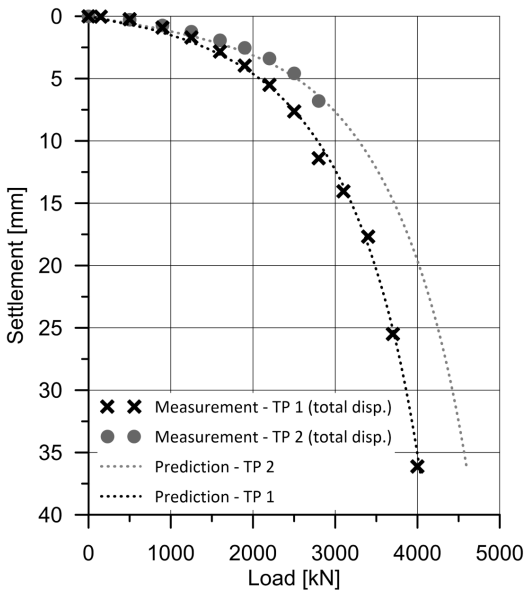

FIGURE 14. Comparison with predictions for both piles.

frictions along both piles are plotted in the right part of this figure. It is obvious that no hammering was recorded at depths of 3 to 4 m in the case of PP3b pile (the pile was only pushed downwards by the hammer due to the low resistance of the surrounding soil). Measured and predicted load-displacement curves are shown in Figure 17. The points of the measured load-displacement curves correspond to the ends of the observation intervals for each loading stage after the acceptance criteria were met. The measured displacement values did not stabilise in the last loading stage. Therefore, the initial measured displacement value and the value 25 mm are plotted for this loading stage. It is obvious that the pile PP3a has a higher ultimate capacity and stiffness during loading which is consistent with the hammering log.

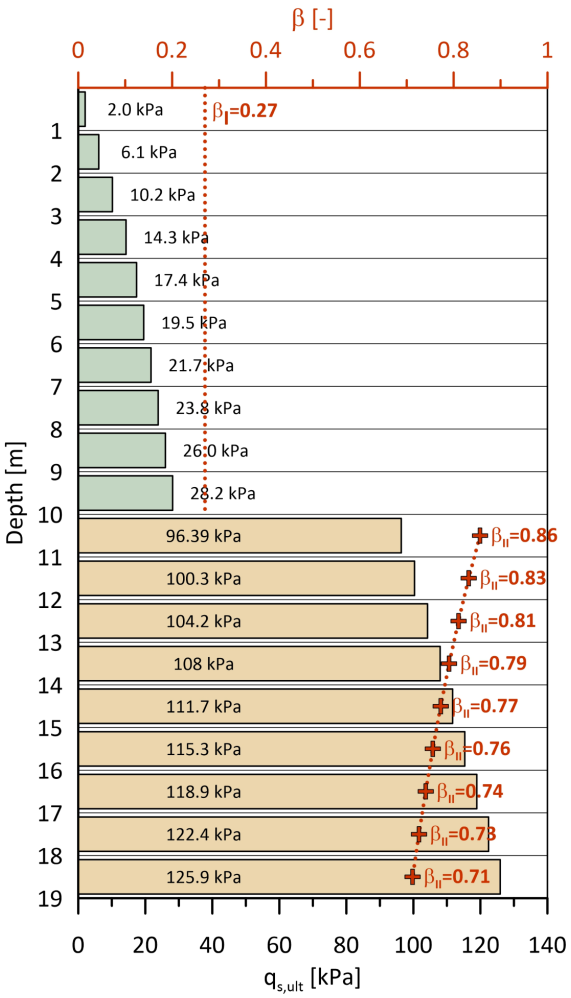

FIGURE 15. Predicted ultimate shaft friction and β factor profiles.

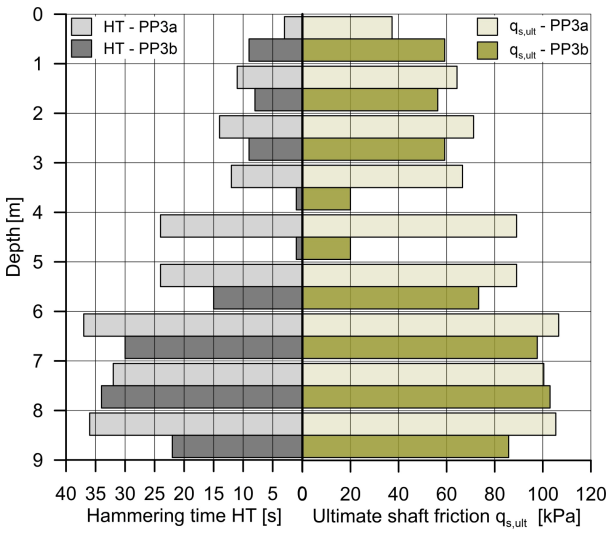

FIGURE 16. Hammering log and predicted ultimate shaft friction profiles for both testing piles.

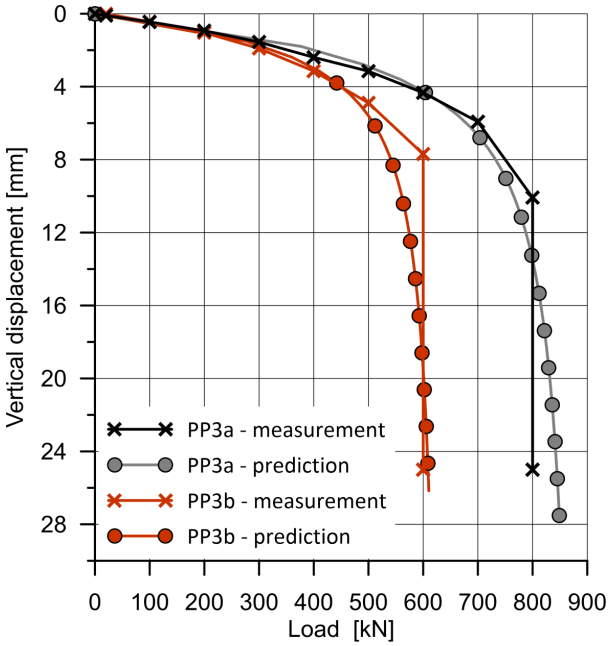

FIGURE 17. Measured and predicted load-displacement curves.

5. CONCLUSION

The paper presents possibilities of using the LTM for two types of deep foundations: large diameter bored piles and driven ductile iron piles. The LTM algorithm begins with a division of an analysed deep foundation into a prescribed number of segments. On each segment, the balance of the external and internal forces is iteratively solved. Thus, the effect of the overall axial stiffness ($\frac{E_p A_p}{L_p}$) on the uniformity of the shaft friction mobilisation is directly incorporated into the solution. Other main advantages of the LTM include: it can be used for both limit states, a larger number of outputs is available (profiles of mobilised shaft friction, ultimate shaft friction, axial force, and axial displacement along a pile). The β method relating the ultimate shaft friction to the effective overburden pressure was used for bored piles. For driven piles, the ultimate shaft friction profile is related directly to the recorded hammering times through the so-called load-transfer coefficients, which also depend on the hammering time. The presented inverse analyses demonstrated that using the LTM and its modifications described in this paper led to good agreement with both the measured load-displacement curve and the axial force (strain) profiles recorded by the resistance gauges.

ACKNOWLEDGEMENTS

The research was supported by the Technology Agency of the Czech Republic under project no. ZETA2-TJ02000140.

REFERENCES

[1] H. G. Poulos, E. H. Davis. *Pile Foundation Analysis and Design.* John Wiley and Sons, New York, USA, 1980.

[2] H. B. Seed, L. C. Reese. The action of soft clay along friction piles. *Transactions of the American Society of*

Civil Engineers **122**(1):731–754, 1957. https://doi.org/10.1061/TACEAT.0007501

[3] E. S. B. Reddy, M. O'Reilly, D. Chapman. A software to predict the behaviour of tension piles. *Computers & Structures* **62**(4):653–658, 1997. https://doi.org/10.1016/S0045-7949(97)80002-3

[4] E. S. B. Reddy, M. O'Reilly, D. N. Chapman. Modified T-Z model – a software for tension piles. *Computers & Structures* **68**(6):613–625, 1998. https://doi.org/10.1016/S0045-7949(98)00089-3

[5] M. F. Randolph, C. P. Wroth. Analysis of deformation of vertically loaded piles. *Journal of the Geotechnical Engineering Division* **104**(12):1465–1488, 1978. https://doi.org/10.1061/AJGEB6.0000729

[6] American Petroleum Institute. RP 2A-WSD: Recommended practice for planning, designing and constructing fixed offshore platforms – working stress design, 2003.

[7] R. Frank, S.-R. Zhao. Estimation à partir des paramètres pressiométriques de l'enfoncement sous charge axiale de pieux forés dans des sols fins [In French; Estimation of parameters from pressuremeter test for determination of displacement of bored piles in fine soils]. *Bulletin de Liaison des Laboratoires des Ponts et Chaussées* (119):17–24, 1982.

[8] W. G. K. Fleming. A new method for signle pile settlement prediction and analysis. *Géotechnique* **42**(3):411–425, 1992. https://doi.org/10.1680/geot.1992.42.3.411

[9] Q.-q. Zhang, Z.-m. Zhang. A simplified nonlinear approach for single pile settlement analysis. *Canadian Geotechnical Journal* **49**(11):1256–1266, 2012. https://doi.org/10.1139/t11-110

[10] C. Bohn, A. L. dos Santos, R. Frank. Development of axial pile load transfer curves based on instrumented load tests. *Journal of Geotechnical and Geoenvironmental Engineering* **143**(1), 2017. https://doi.org/10.1061/(ASCE)GT.1943-5606.0001579

[11] Keller Grundbau Ges.mbH, 2024. [2024-04-26]. https://www.kellergrundbau.at

[12] J. Zahrada. *Loading test of the pile – report, pile 1 200 mm, D 47, SO 210 [In Czech].* Special foundation centre SKANSKA a. s., 2005. Unpublished.

[13] J. Chalmovský. Application of the load-transfer method for predicting the behaviour of deep foundations in the Czech Republic [In Czech], 2021. [2024-09-05]. https://geotech.fce.vutbr.cz/wp-content/uploads/sites/17/2021/01/Vyu%C5%BEit%C3%AD_MPF_%C4%8CR.pdf

[14] German Geotechnical Society. *Recommendations on piling (EA-Pfähle).* Wiley, Berlin, Germany, 2013. https://doi.org/10.1002/9783433604113

[15] J. Hulla, P. Turček. *Zakladanie stavieb [In Slovak; Foundation of structures].* Jaga group, 1998.

[16] J. Burland. Shaft friction of piles in clay – a simple fundamental approach. *Ground Engineering* **6**(3):30–42, 1973.

[17] F. K. Chin. The inverse slope as a prediction of ultimate bearing capacity of piles. In *Proceedings of the 3rd Southeast Asian Conference on Soil Engineering*, pp. 83–91. 1972.

[18] F. H. Kulhawy, P. Mayne. *Manual on Estimating Soil Properties for Foundation Design.* Cornell University, Geotechnical Enineering Group, Ithaca, New York, USA, 1990.